Interface Magnetic Anisotropy in Epitaxial Superlattices

Brad N. Engel, Craig D. England, Robert A. Van Leeuwen, Michael H. Wiedmann, and Charles M. Falco
Department of Physics and Optical Sciences Center, University of Arizona, Tucson, Arizona 85721
(Received 3 April 1991)

We have studied the uniaxial magnetic anisotropy of Co/Pd superlattices grown under identical conditions by molecular-beam epitaxy along the three crystal axes: [001], [110], and [111]. Our measurements unambiguously demonstrate that the large systematic variations of the anisotropy energy with crystal orientation result solely from differences in the volume contribution to the anisotropy. We find the perpendicular interface anisotropy to be *independent* of the epitaxial orientation (0.63 ± 0.05 erg/cm^2), and hence to be an intrinsic property of the Co/Pd interface.

PACS numbers: 75.50.Rr, 75.30.Gw, 75.70.Cn

Since its first prediction [1] and eventual experimental observation [2], the mechanism responsible for the magnetic anisotropy resulting from a free surface or interface has remained an unsolved problem in magnetism. Mainly because of large variations in thin-film deposition conditions and techniques, the isolation of a fundamental underlying mechanism of interface anisotropy has been difficult. Unfortunately, complicating factors such as the microstructure, impurity amounts, and interdiffusion are not easily incorporated into present theoretical models [3–5] that are based on ideal systems containing atomically perfect interfaces. However, with recent advances in molecular-beam-epitaxy (MBE) techniques, it has become possible to produce high-quality crystalline magnetic films that closely approximate the ideal case treated by present theory.

In order to uniquely determine the role of crystal structure in interfacial magnetic anisotropy, we have used MBE to grow a series of Co/Pd superlattices aligned along the three high-symmetry crystal axes: [001], [110], and [111]. In addition to the fifteen epitaxial samples, a companion set of six polycrystalline Co/Pd multilayers was simultaneously deposited onto Si(111) substrates for direct comparisons. Identical conditions (substrate temperature, evaporation rate, and background pressure) were maintained during deposition of each of the 21 films grown for the present study, in an effort to minimize differences in interface diffusion and impurity levels. The Pd layer thickness for all samples was held fixed at $t_{Pd} = 10 \pm 1$ Å, and t_{Co} was systematically varied for each orientation to allow a clear separation of the interfacial and volume contributions to the total magnetic anisotropy. The magnetic properties of these samples were studied by a combination of vibrating-sample, SQUID, and torque magnetometry, resulting in a detailed study of the structural dependence of magnetic anisotropy in a systematically prepared and characterized metallic superlattice system.

Previous evidence for an orientational dependence of the uniaxial magnetic anisotropy in superlattices has been reported for Co/Pd [6] and Co/Pt [7]. In the case of Co/Pd [6], large differences were observed between (111) textured polycrystalline films deposited on glass and (001) epitaxial superlattices evaporated on NaCl. Decreasing the Co layer thickness, the authors found a crossover from in-plane to perpendicular behavior for the (001) samples between 1 and 2 atomic layers (~3 Å). This is in marked contrast to their (111) textured films, which became perpendicular at 6 atomic layers (~12 Å).

Recently, the MBE growth of several Co/Pt superlattices along the [001], [110], and [111] directions was reported [7]. Hysteresis curves measured by polar Kerr rotation were presented for one sample of each orientation, with identical design parameters, (3 Å Co)/(16 Å Pt). Although the uniaxial anisotropy was not determined, large variations in the loop behavior indicated an easy plane for the (001) sample and a perpendicular easy axis for the (111) and (110) superlattices. These results clearly indicate the usefulness of the study of epitaxial superlattices for addressing the magnetic anisotropy problem.

To prepare suitable single-crystal starting surfaces for growth of the Co/Pd superlattices in the three orientations for the present study, we employed a variation of recently reported seeded-epitaxy techniques used in the growth of fcc metals on GaAs [7,8]. Briefly, 2.5 cm × 5 cm GaAs (110) and (001) wafers were indium bonded to the center of 7.5-cm-diam Si(111) wafers. The exposed regions of these Si wafers served as substrates for "companion" polycrystalline multilayers, with which the total Co content of each superlattice was accurately determined ($\pm 3\%$) by Rutherford backscattering spectrometry (RBS). Sample rotation during deposition assured thickness variations of less than 1% across the full substrate diameter as determined by RBS.

After heating in UHV (~10^{-10} torr) at 625 °C for 30 min, the substrates were cooled to room temperature, resulting in clean, smooth, well-ordered GaAs surfaces for deposition as determined by *in situ* reflection high-energy and low-energy electron diffraction (RHEED and LEED). The Co was evaporated from an electron beam gun at a constant rate of 0.25 Å/s which was maintained by optical-feedback regulation of the power. The Pd was evaporated from a high-temperature effusion cell regulated at 1400 °C, providing a constant rate of 0.1 Å/s at the substrate. The background pressure during deposition

was $\leq 5\times10^{-10}$ torr.

The oriented growth of the superlattices was provided by initial deposition of epitaxial Co, Pd, and Ag buffer layers. RHEED and LEED were used to determine the crystal symmetry and quality during growth. *Ex situ* scanning tunneling microscopy (STM) along with high- and low-angle x-ray diffraction were employed to determine the surface morphology and crystal structure for each of the samples.

To grow the [111]-oriented Co/Pd superlattices, we first deposited a 6-Å layer of Co onto GaAs(110), followed by a 500-Å layer of Pd. RHEED and LEED indicated that the fcc (111) symmetry of this starting surface was maintained throughout the superlattice growth. STM images of the final surface reveal ~500-Å-diam grains with ~4-Å peak-to-peak height variations across their top. The individual grains are separated by ~50-Å-wide by ~50-Å-deep valleys.

The (001) superlattices were produced by first depositing 6–10 Å of Co on GaAs(001), followed by 500 Å of Ag which was evaporated at 1 Å/s from a second electron beam gun. RHEED and LEED indicated that the fcc (001) orientation was preserved throughout the superlattice growth. The crystal quality and morphology of these superlattices was very similar to the (111) samples, displaying comparable electron-diffraction sharpness and ~1000-Å-diam flat grains as measured by STM.

For (110) growth, a buffer layer of 400 Å of Ag followed by 200 Å of Pd was deposited directly onto room-temperature GaAs(001) substrates providing an fcc (110) structure for the resultant superlattices. RHEED and LEED patterns indicated well-ordered growth along the [110] azimuthal direction. However, the patterns along the [100] azimuthal direction were less distinct, with a stronger diffuse background. STM images of the final surface reveal large, flat patches of ~4000 Å extent separated by ~200-Å-deep by ~1000-Å-wide valleys.

High-angle x-ray-diffraction scans displayed only the allowed fcc (111), (200), and (220) reflections for the [111]-, [100]-, and [110]-oriented superlattices, respectively. Because of the perpendicular scattering geometry, the stacking sequence (hcp or fcc) of the (111) samples could not be uniquely determined. Narrow linewidths, consistent with large perpendicular coherence lengths ($T/2\leq\xi\leq T$, where T is the total film thickness), were found for all of the epitaxial superlattices. Rocking curves performed on the first superlattice Bragg reflection of these films display a full width at half maximum (FWHM) of $\leq 2°$, indicating well-oriented, single-crystal structures. In contrast, the companion polycrystalline multilayers show a (111) texture with ~15° FWHM rocking curves and structural coherence lengths of only ~100 Å.

Because of the low x-ray contrast between Co and Pd and the small modulation periods studied, we were unable to observe more than one low-angle diffraction peak for a majority of our samples. However, the falloff in intensity with increasing grazing angle was very similar for samples of identical layer thicknesses, suggesting only small differences in interface roughness and interdiffusion for the different crystal orientations. High-intensity synchrotron x-ray studies are in progress to allow detailed modeling of the interface quality in the three orientations, and will be reported elsewhere.

Room-temperature hysteresis curves to 17 kOe of ~6×6 mm sections of each superlattice were measured by vibrating-sample magnetometry (VSM) at both perpendicular and parallel orientations with respect to the film plane. For one sample with an extremely large anisotropy (2 Å Co, [111]), a SQUID magnetometer was used to measure the moment to 55 kOe. The quantity $M\Lambda$, where M is the total magnetization and Λ is the bilayer period ($\Lambda=t_{Co}+t_{Pd}$), was determined directly from the expression $M\Lambda=I/NA$. Here, I is the measured magnetic moment, N is the total number of bilayers, and A is the area of the film determined from digitized micrographs for each sample.

Large enhancements of the magnetization arising from Pd polarization have been previously observed in Co/Pd multilayers [6,9], and are observed in our samples as well. Figure 1 is a plot of the saturation magnetization versus Co thickness of our epitaxial superlattices. The linear behavior of this figure is well described by

$$M_s\Lambda=M_{Co}t_{Co}+M_{Pd}t_{Pd}^{eff}, \quad (1)$$

where M_{Co} is the intrinsic Co magnetization, t_{Co} is the Co layer thickness, M_{Pd} is the effective magnetization of the polarized Pd, and t_{Pd}^{eff} is the effective layer thickness of polarized Pd. Thus, the intrinsic magnetization of the Co

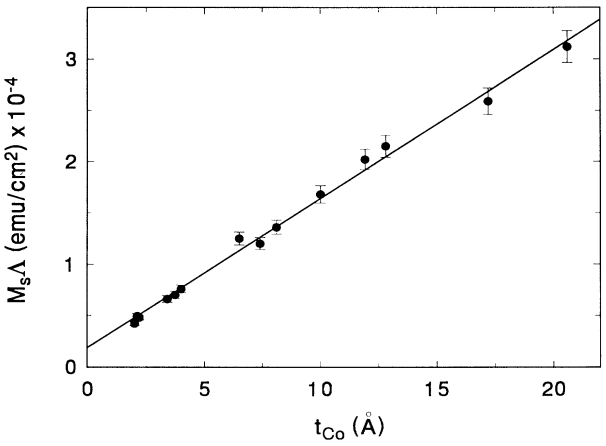

FIG. 1. The Co-thickness dependence of the total saturation magnetization multiplied by the superlattice period. From the model described in the text, the slope of the linear fit gives the intrinsic magnetization of the Co layers as $M_{Co}=1460\pm40$ emu/cm^3.

layers, separated from enhancement effects due to the Pd, can be obtained from the slope of the linear fit. We find $M_{Co}=1460\pm40$ emu/cm^3. Within experimental error, this value is identical to the quoted value of 1422 emu/cm^3 for bulk, hcp Co [10].

Very large anisotropies were observed in several of the superlattices, preventing saturation along the hard direction in fields as high as 55 kOe. For these samples, the moderate fields available in conventional torque magnetometers (≈ 20 kOe) make determination of the anisotropy constants difficult. Instead, we have employed a technique developed by Sucksmith and Thompson [11] that involves analyzing the magnitude and curvature of the hard-axis magnetization as a function of applied field. Saturation of the spins in the hard direction is not required, allowing an accurate determination of the uniaxial anisotropy constants K_1 and K_2 in easily obtainable fields. The two sections of each hysteresis loop were averaged at constant magnetization values and fits with the model [11] were performed above the coercive field. Figure 2 displays the hard-axis magnetization measured to high field of a strongly perpendicular superlattice ($t_{Co}=2$ Å, [111]). The solid curve is a fit by the model, demonstrating excellent agreement over the entire range. We have verified the results obtained from this technique by making direct comparisons to torque magnetometry for several samples, and find agreement to better than 10%.

The uniaxial anisotropy energy density ($K_u=K_1+K_2$) for Co/Pd superlattices can be modeled phenomenologically by the inclusion of an effective interface contribution, proportional to $1/t_{Co}$, and a volume term, independent of t_{Co}. To display the $1/t_{Co}$ behavior more clearly, the product of the anisotropy energy per Co volume and the Co layer thickness can be written as

$$K_u^{Co}t_{Co}=(K_v^{eff}-2\pi M_s^2)t_{Co}+2K_s\,, \qquad (2)$$

where $K_v^{eff}=K_{mc}+K_{me}$ is the sum of the magnetocrystalline and magnetoelastic contributions, $2\pi M_s^2$ is the shape anisotropy of a uniform sheet of bulk Co, and K_s is the interface anisotropy energy density. The factor of 2 in the last term accounts for the two interfaces per magnetic layer. In this convention, $K_u>0$ for a perpendicular easy axis. The minus sign of the shape anisotropy term therefore indicates its tendency to favor in-plane behavior. An estimate of the additional shape anisotropy from the polarized Pd was found to be an insignificant contribution and therefore not included in the analysis.

From Eq. (2), the product $K_u^{Co}t_{Co}$ should be linear in t_{Co} with a slope of $K_v^{eff}-2\pi M_s^2$ and an intercept of $2K_s$. This quantity, $K_u^{Co}t_{Co}=K_u^{tot}\Lambda$, is directly determined from the hard-axis magnetization curves of our superlattices, $M(H)\Lambda$. Figure 3 displays $K_u^{Co}t_{Co}$ vs t_{Co} for all three crystal orientations and the polycrystalline multilayers. The estimated uncertainty from known sources is within the size of the data points except for the $t_{Co}=8$ Å, [110] sample that was measured with torque magnetometry. The behavior is seen to be linear for all sets of samples as expected from Eq. (2).

The most striking feature of Fig. 3 is the convergence of all curves to a single intercept, $2K_s$. These results show that the contribution of the Co-Pd interface to the total anisotropy, *independent* of crystal orientation and epitaxy, is $K_s=0.63\pm0.05$ erg/cm^2 for multilayers deposited under these conditions. However, as would be expected, growth along the different crystal axes produces very different magnetocrystalline and magnetoelastic contributions. As indicated by the slopes of the data, the large variations with t_{Co} of the total anisotropy energy are solely a result of greatly different volume contributions.

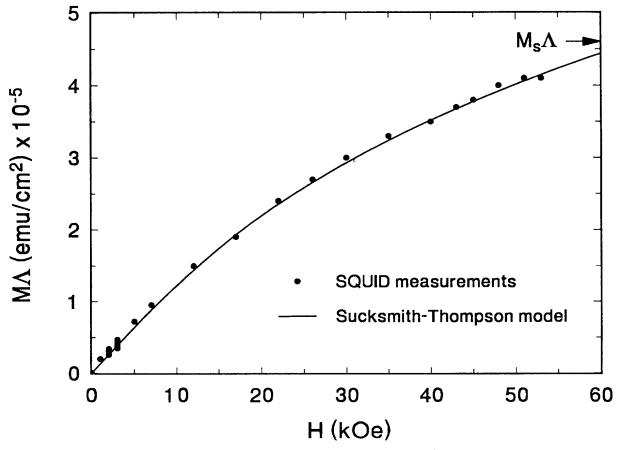

FIG. 2. In-plane (hard-axis) magnetization of the [(2 Å Co)/(11 Å Pd)]×50, [111]-oriented superlattice. The solid curve is a fit with the model as described in the text, and provides the anisotropy constants K_1 and K_2.

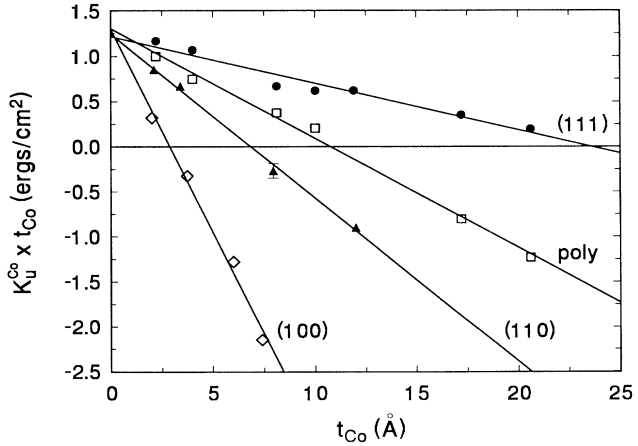

FIG. 3. The uniaxial anisotropy energy times the Co thickness vs Co thickness for all 21 of the epitaxial and polycrystalline samples. The convergence of the four curves at $t_{Co}=0$ indicates an identical interface anisotropy, independent of orientation ($K_s=0.63\pm0.05$ erg/cm^2).

The anisotropy measurements of our polycrystalline samples agree well with other similarly prepared multilayers reported in the literature [6], and show a crossover to in-plane behavior at $t_{Co}=11$ Å. To within our experimental precision, there is no evidence of an effective volume contribution. The anisotropy behavior of these films is dominated by the shape and interface contributions.

The most strongly perpendicular superlattices are the (111) series, which show a crossover to in-plane behavior for $t_{Co}>24$ Å. Since the [111] direction (c axis for hcp) is the easy axis for a bulk Co crystal, the magnetocrystalline contribution can aid the perpendicular anisotropy for films oriented along this direction. Correcting for the shape anisotropy ($2\pi M_s^2=1.27\times10^7$ ergs/cm^3) gives an effective volume anisotropy of $K_v^{\text{eff}}=(7.7\pm0.1)\times10^6$ ergs/cm^3. This value is about 20% larger than the magnetocrystalline anisotropy for a bulk, single crystal of hcp Co (6.3×10^6 ergs/cm^3) [11], suggesting a positive magnetoelastic contribution. Analysis of our x-ray-diffraction measurements [12] and recent high-resolution RHEED measurements [13] of Co grown on a Pd(111) surface indicate no appreciable coherent strain arising from the 9% lattice mismatch. However, because the magnetostriction constants of hcp Co are very large, the existence of as little as 0.2% in-plane tensile strain of the Co could cause the additional positive magnetoelastic energy we observe.

In sharp contrast to the (111) orientation, the (001) superlattices show a crossover to in-plane behavior between one and two atomic layers of Co; $t_{Co}=3$ Å. This is consistent with measurements of Co/Pd (001) superlattices grown on NaCl [6]. This very large in-plane volume anisotropy, $K_v^{\text{eff}}=(-3.2\pm0.3)\times10^7$ ergs/cm^3, is an order of magnitude larger than any of the relevant magnetocrystalline contributions and therefore is most likely of magnetoelastic origin. Both our x-ray-diffraction measurements of these superlattices [12] and transmission-electron-diffraction measurements of Co/Pd multilayers deposited on NaCl [6] indicate the existence of a large coherent strain for epitaxial samples grown in this orientation. We have estimated the magnetoelastic energy from our measured lattice strain and the magnetostriction constant of fcc Co and find very good agreement with our measured volume anisotropy [12]. These (001) superlattices simultaneously display both a large, in-plane magnetoelastic contribution and an orientation-independent perpendicular interface anisotropy. This casts doubt on the recently predicted [14] role of interfacial strain as a cause of perpendicular interface anisotropy.

The (110) superlattices display an intermediate behavior, with a crossover of 7 Å. Because of the rectangular symmetry of the (110) face, we observe an additional cubic anisotropy when the spins are tipped into the film plane. Hence, for the perpendicular superlattices, care was taken to align this cubic axis along the magnetic field for proper determination of the uniaxial anisotropy from the hard-axis loops. This cubic anisotropy also complicates the hard-axis loop shape for the $t_{Co}=8$ Å sample, where the uniaxial contribution is small. Torque magnetometry was therefore used to determine the anisotropy for this superlattice.

In conclusion, by carefully growing and characterizing fifteen epitaxial and six polycrystalline Co/Pd samples under identical conditions, we have demonstrated that the perpendicular magnetic interface anisotropy in a metallic multilayer system is *independent* of crystal structure. The large variations of the uniaxial anisotropy energy we observe with crystal orientation are a result of volume terms that can be accounted for by magnetocrystalline and magnetoelastic contributions. The constant magnitude of the interface contribution is difficult to explain in light of the variations in surface density associated with the different crystal orientations. The presence of a large in-plane magnetoelastic contribution for the (001) films brings into question the role of interfacial strain in the mechanism of perpendicular anisotropy for the Co/Pd system. The structural dependence of the magnetic anisotropy deduced from this present work will provide a rigorous test for theoretical explanations of the magnetic anisotropy in metallic superlattices.

We gratefully acknowledge J. Slaughter for many useful discussions, J. Leavitt and L. McIntyre for the RBS measurements, V. Harzer, B. Hillebrands, and G. Güntherodt for the SQUID measurements, and C. Brucker for the torque measurements. This work was supported by the University of Arizona Optical Data Storage Center and the U.S. Department of Energy Grant No. DE-FG02-87ER45297.

[1] L. Néel, J. Phys. Radium **15**, 376 (1954).
[2] U. Gradmann, Appl. Phys. **3**, 161 (1974).
[3] J. G. Gay and R. Richter, Phys. Rev. Lett. **56**, 2728 (1986).
[4] C. Li, A. J. Freeman, and C. L. Fu, J. Magn. Magn. Mater. **83**, 51 (1990).
[5] G. H. O. Daalderop, P. J. Kelly, and M. F. H. Schuurmans, Phys. Rev. B **42**, 7270 (1990).
[6] F. J. A. den Broeder, D. Kuiper, H. C. Donkersloot, and W. Hoving, Appl. Phys. A **49**, 507 (1989).
[7] C. H. Lee, R. F. C. Farrow, C. J. Lin, E. E. Marinero, and C. J. Chien, Phys. Rev. B **42**, 11 384 (1990).
[8] C. H. Lee, H. He, F. Lamelas, W. Vavra, C. Uher, and R. Clarke, Phys. Rev. Lett. **62**, 653 (1989).
[9] P. F. Carcia, A. Suna, D. G. Onn, and R. van Antwerp, Superlattices Microstruct. **1**, 101 (1985).
[10] *American Institute of Physics Handbook* (McGraw-Hill, New York, 1963), 2nd ed.
[11] W. Sucksmith and J. E. Thompson, Proc. Roy. Soc. London A **225**, 362 (1954).
[12] Quantitative details of this analysis are presented in B. N. Engel, C. D. England, R. Van Leeuwen, M. Wiedmann, and C. M. Falco, in Proceedings of MMM-Intermag 91 [J. Appl. Phys. (to be published)].
[13] S. T. Purcell, H. W. van Kesteren, E. C. Cosman, and W. Hoving, J. Magn. Magn. Mater. **93**, 25 (1991).
[14] P. Bruno and J.-P. Renard, Appl. Phys. A **49**, 499 (1989).